*J. Phys. Chem.* **1990**, *94*, 2730-2734

# In Situ Solid-State NMR Studies of the Catalytic Conversion of Methanol on the Molecular Sieve SAPO-34

**Michael W. Anderson, Bogdan Sulikowski,[†] Patrick J. Barrie, and Jacek Klinowski***

*Department of Chemistry, University of Cambridge, Lensfield Road, Cambridge CB2 1EW, U.K.*

*(Received: November 2, 1989)*

We have monitored the shape-selective catalytic conversion of methanol (MeOH) to low-molecular-weight olefins and aliphatics over the molecular sieve SAPO-34 using $^{13}$C and $^{1}$H magic-angle-spinning (MAS) NMR in tandem with gas chromatography. The size of the eight-membered windows in the structure limits the gas-phase products to linear $C_1$, $C_2$, and $C_3$ species. However, the main species present *in the intracrystalline space* are branched $C_4$ and $C_5$ saturated hydrocarbons such as isobutane and isopentane: too large to leave the intracrystalline pore system they become trapped, thus imposing an additional steric constraint on the diffusion of linear hydrocarbons. This favors the diffusion of $C_1$ and $C_2$ species out of the crystallites and is responsible for the apparent overall selectivity of SAPO-34 for ethylene. By contrast, intracrystalline chemistry favors the formation of propylene. Unlike on zeolite H-ZSM-5, no carbon monoxide intermediate and no aromatics are formed. We suggest modifications to the zeolite composition designed to make the zeolite more selective for $C_3$ rather than $C_2$ species.

## Introduction

The declining world oil reserves have stimulated considerable efforts toward the exploration of alternative sources of energy and organic chemicals. One answer is to use the abundant supply of coal as a source of synthesis gas ($CO + H_2$), which is readily converted to methanol (MeOH).[1] MeOH can then be transformed into higher molecular weight hydrocarbons (olefins, aliphatics, and aromatics) over shape-selective zeolite catalysts, the most successful of which in this respect is H-ZSM-5 capable of converting MeOH at 370 °C to hydrocarbons up to $C_{10}$.[2] The selective synthesis of ethylene and propylene, the key intermediates for the production of detergents, plasticizers, lubricants, and a variety of chemicals, proceeds over smaller pore zeolites such as chabazite and erionite.[3-5]

Since 1982 several new families of porous solids have been synthesized. $AlPO_4$ molecular sieves, built from alternating $AlO_4$ and $PO_4$ tetrahedra and prepared under mild hydrothermal conditions from gels containing sources of aluminum, phosphorus, and a structure-directing template, were the first to be discovered. Incorporation of a silicon source into an aluminophosphate gel results in the formation of silicoaluminophosphates, known as SAPOs, and the incorporation of a metal, M (such as Mg, Mn, Fe, Co, or Zn), into $AlPO_4$ and SAPO gives the MAPO and MAPSO sieves, respectively. Some SAPO, MAPO, and MAPSO compounds have high Brønsted acidities and a considerable potential as catalysts, ion exchangers, and molecular sieves.

The molecular sieve SAPO-34,[6,7] which has the framework topolog of the natural zeolite chabazite (Figure 1), has been shown[8-11] to convert MeOH to hydrocarbons with a selectivity for $C_2$ of 33.8 mol %. We have demonstrated[12,13] that the course of catalytic reactions on molecular sieves can be quantitatively studied using in situ $^{13}$C and $^{1}$H MAS NMR (which monitors the species adsorbed in the intracrystalline space). In the reaction of MeOH over zeolite H-ZSM-5 we identified a number of aliphatic and aromatic species in the adsorbed phase, monitored their fate during the course of the reaction, and compared the composition of the adsorbed phase with that of the gaseous products leaving the catalyst. We have also observed directly, for the first time, different kinds of shape selectivity and identified CO as an intermediate.

We now describe the application of the technique to the conversion of MeOH over SAPO-34. In what follows, we shall refer to the gas species leaving the catalyst (and monitored by gas chromatography) as "products" and the compounds monitored by NMR in the intracrystalline space as the "adsorbed phase".

## Experimental Section

A sample of SAPO-34 was prepared based on the methods described in the original patent[14] from a gel of composition $Al_2O_3$:$P_2O_5$:0.6$SiO_2$:$(TEA)_2O$:0.5$n$-$Pr_2NH$:50$H_2O$. The sources of the framework elements were pseudoboehmite, 85% phosphoric acid, and Cab-o-Sil fumed silica. The gel was crystallized in a Teflon-lined autoclave at 200 °C for 40 h. X-ray diffraction (XRD) shows that the product is pure and highly crystalline. Chemical analysis by atomic absorption gave an Al/Si ratio of 6. Assuming that all Si substitutes onto P sites of the equivalent $AlPO_4$ structure (see below), this corresponds to an approximate chemical composition of $SiAl_6P_5O_{24}$. Figure 2 shows the powder diffractogram of as-synthesized SAPO-34. The material exhibits rhombohedral symmetry with lattice parameters $a = b = c = 9.346$ Å and $\alpha = \beta = \gamma = 94.99°$. The product was calcined at 500 °C for 12 h to remove the organic templates prior to catalytic testing. Calcination caused only a slight loss of crystallinity.

$^{29}$Si, $^{31}$P, and $^{27}$Al MAS NMR spectra were recorded with a Bruker MSL-400 spectrometer at 79.49, 161.98, and 104.26 MHz, respectively. Spinning speeds of 2.5 kHz were used for $^{29}$Si and 4.5 kHz for $^{31}$P and $^{27}$Al. Recycle times were 15, 5, and 0.2 s for $^{29}$Si, $^{31}$P and $^{27}$Al, respectively, and chemical shifts are quoted from TMS, 85% phosphoric acid, and $Al(H_2O)_6^{3+}$. Short $\pi/20$ radio-frequency pulses were used for $^{27}$Al spectra to ensure that they are quantitatively reliable.[16,17]

---

[†] On leave from the Institute of Organic Chemistry and Technology, Krakôw Technical University, 31-155 Krakôw, Poland.

(1) Maj, J. J.; Colmenares, C.; Somorjai, G. A. *Appl. Catal.* **1984**, *10*, 313.

(2) Meisel, S. L.; McCullough, J. P.; Weisz, P. B. *CHEMTECH* **1976**, *6*, 86.

(3) Chang, C. D.; Lang, W. H.; Silvestri, A. J. U.S. Patent 4,062,095, 1978.

(4) Singh, B. B.; Lin, F. N.; Anthony, R. G. *Chem. Eng. Commun.* **1980**, *4*, 749.

(5) Wunder, F. A.; Leupold, E. I. *Angew. Chem., Int. Ed. Engl.* **1980**, *19*, 126.

(6) Lok, B. M.; Messina, C. A.; Patton, R. L.; Gajek, R. T.; Cannan, T. R.; Flanigen, E. M. *J. Am. Chem. Soc.* **1984**, *106*, 6092.

(7) Ito, M.; Shimoyama, Y.; Saito, Y.; Tsurita, Y.; Otake, M. *Acta Crystallogr.* **1985**, *C41*, 1698.

(8) Kaiser, S. W. *Arab. J. Sci. Eng.* **1985**, *10*, 361.

(9) Kaiser, S. W. Eur. Pat. Appl. 105,512, 1984.

(10) Kaiser, S. W. U.S. Patent 4,524,234, 1985.

(11) Hongyuan, L.; Liang, J.; Liu, Z.; Zhao, S.; Wang, R. *Cuihua Xuebao* **1988**, *9*, 87.

(12) Anderson, M. W.; Klinowski, J. *Nature* **1989**, *339*, 200.

(13) Anderson, M. W.; Klinowski, J. *J. Am. Chem. Soc.* **1990**, *112*, 10.

(14) Lok, B. M.; Messina, C. A.; Patton, R. L.; Gajek, R. T.; Cannan, T. R.; Flanigen, E. M. U.S. Patent 4,440,871, 1984.

(15) Engelhardt, G.; Michel, D. *High-Resolution Solid-State NMR of Silicates and Zeolites*; Wiley: Chichester, 1987.

(16) Samoson, A. Lippmaa, E. *Phys. Rev.* **1983**, *B28*, 6567; *Chem. Phys. Lett.* **1983**, *100*, 205.

0022-3654/90/2094-2730$02.50/0 © 1990 American Chemical Society

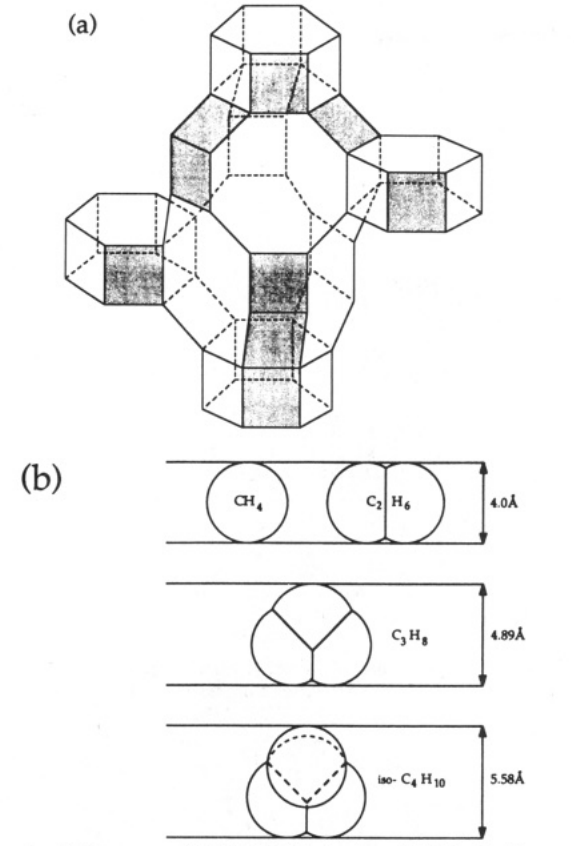

**Figure 1.** (a) Structure of SAPO-34/chabazite. (b) Kinetic diameters of relevant aliphatic molecules (adapted from ref 29).

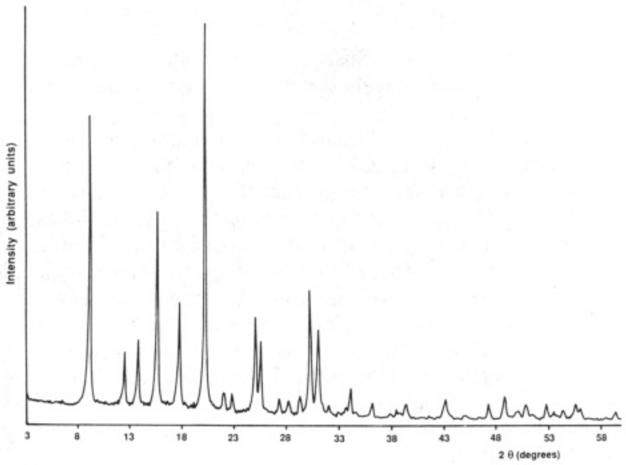

**Figure 2.** X-ray powder diffractogram of as-synthesized SAPO-34 measured using a Philips PW1710 automatic powder diffractometer with a vertical goniometer. Cu K$\alpha$ radiation was selected by a graphite monochromatoor in the diffracted beam. Unit cell parameters were calculated with silicon powder as an internal standard.

Catalytic tests were performed in a microreactor operating in a pulse mode. The sample was first calcined in air at 500 °C, pelletized without binder, crushed, and sieved to 30–60 mesh. A 100-mg sample was diluted with 3 g of quartz chips, packed into a stainless steel down-flow microreactor (10-mm i.d.) placed in a tube furnace. The thermocouple well was located centrally in the microreactor connected to a gas chromatograph. The catalyst was activated overnight at 450 °C in a helium flow. Methanol was passed through the catalyst bed, and the reaction products were conveyed at 200 °C to a gas sample valve. Products were analyzed by use of a high-resolution gas chromatograph (Carlo Erba Mega 5340) using the DB-1 fused silica capillary column (30 m × 0.317 mm) and a flame-ionization detector. Analytical grade hydrocarbons and MeOH supplied by Aldrich were used without further purification.

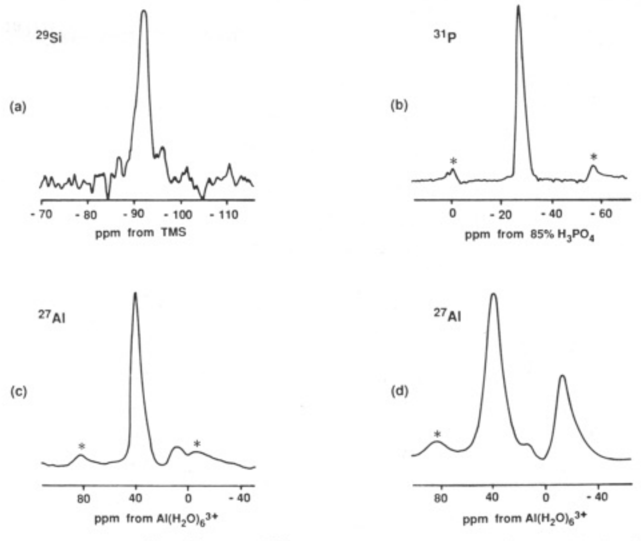

**Figure 3.** (a–c) $^{29}$Si, $^{31}$P, and $^{27}$Al MAS NMR spectra of as-synthesized SAPO-34 and (d) the $^{27}$Al spectrum of the calcined form.

MeOH 99% enriched in $^{13}$C was diluted to 30 wt % with ordinary MeOH and purified by the freeze–pump–thaw method. Catalyst samples for $^{13}$C MAS NMR were placed in specially designed Pyrex microreactors,[12,18] in which they were activated, charged with methanol, sealed off, and heated to the desired reaction temperature without exposure to the atmosphere. They were then quenched by immersion in liquid nitrogen in order to stop the reaction and inserted into zirconia MAS rotors. All $^{13}$C NMR spectra were recorded at ambient temperature by using high-power proton decoupling, both with and without cross-polarization. High-power decoupling experiments were carried out with 40° $^{13}$C pulses and a 10-s repetition time. Spin–lattice relaxation times were measured to ensure that the repetition times were adequate to give quantitatively reliable spectra. $^{13}$C chemical shifts are referred to external tetramethylsilane (TMS).

## Results

$^{29}$Si and $^{31}$P MAS NMR spectra of SAPO-34 (Figure 3) each show a single resonance at −91.8 and −28.5 ppm, respectively, typical of Si(4Al) and P(4Al) environments in $AlPO_4$ and SAPO materials, respectively.[19–21] The absence of a $^{29}$Si signal in the −110 ppm region shows that no amorphous silica is present and also rules out the presence of silica-rich regions within the framework, although these have been suggested for some SAPO structures by other workers.[22,23] The unique Si and P environments show that all the silicon is incorporated into the P framework positions of the equivalent hypothetical $AlPO_4$ structure. Each Si atom induces a negative framework charge, which in the calcined form is balanced by an acidic proton. Since one in every six phosphorus atoms in the framework of our sample have been substituted by Si, there is thus approximately one Brønsted acid site per cage. This is much less than in H–chabazite, where for a typical composition with Si/Al = 2 there are four Al atoms (and thus four Brønsted sites) per cage.

The $^{27}$Al MAS NMR spectra show that in the as-prepared SAPO-34 most of the Al is in a tetrahedral environment (at 39.0 ppm). Calcination results in the formation of a significant amount

---

(17) Man, P. P.; Klinowski, J.; Trokiner, A.; Zanni, H.; Papon, P. *Chem. Phys. Lett.* **1988**, *151*, 143.

(18) Carpenter, T. A.; Klinowski, J.; Tennakoon, D. T. B.; Smith, C. J.; Edwards, D. C. *J. Magn. Reson.* **1986**, *68*, 561.

(19) Blackwell, C. S.; Patton, R. L. *J. Phys. Chem.* **1984**, *88*, 6135.

(20) Appleyard, I. P.; Harris, R. K.; Fitch, F. R. *Chem. Lett.* **1985**, 1747.

(21) Blackwell, C. S.; Patton, R. L. *J. Phys. Chem.* **1988**, *92*, 3965.

(22) Martens, J. A.; Mertens, M.; Grobet, P. J.; Jacobs, P. A. In *Innovation in Zeolite Materials Science*; Grobet, P. J., Mortier, W. J., Vansant, E. F., Schulz-Ekloff, G. Eds.; Stud. Surf. Sci. Catal., Vol. 37, Elsevier: Amsterdam, 1988; p 97.

(23) Hasha, D.; de Saldarriaga, L. S.; Hathaway, P. E.; Cox, D. F.; Davis, M. E. *J. Am. Chem. Soc.* **1988**, *110*, 2127.

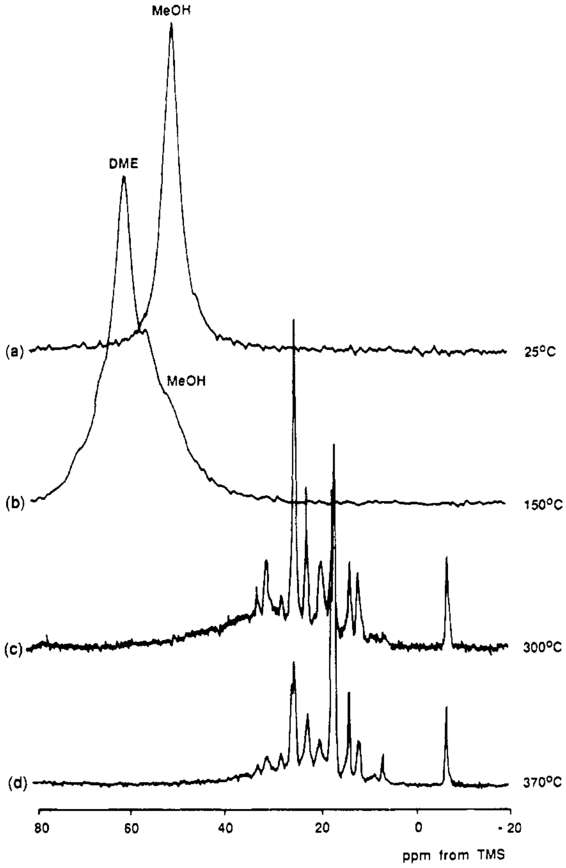

**Figure 4.** $^{13}C$ MAS NMR spectra, with high-power proton decoupling, of the samples: (a) after adsorption of methanol and no thermal treatment; (b) after heating to 150 °C; (c) after heating to 300 °C for 15 min; (d) after heating to 370 °C for 10 min.

of 6-coordinated Al (resonating at −13 ppm) in the hydrated sample. This does not imply that aluminum has been removed from the framework; in a number of $AlPO_4$-based structures Al has been found to have higher coordinations than four due to extra linkages to −OH groups deriving from either the template or the hydrolysis of water.[24] Blackwell and Patton[21] have assigned 6-coordinated Al in calcined and rehydrated SAPO-34 to framework positions and demonstrated that the dehydrated calcined form contains only tetrahedral Al. We note that 6-coordinated Al may contribute to catalytic activity by generating very weak Brønsted acidity. Our $^{29}Si$ and $^{31}P$ MAS NMR spectra change very little upon sample calcination.

Figure 4 shows the $^{13}C$ MAS NMR spectra recorded after reaction at different temperatures. After adsorption of MeOH and no thermal treatment, a single signal at 50 ppm from TMS is observed (Figure 4a) with a full width at half-maximum (fwhm) of ca. 300 Hz. After heating to 150 °C a rather poorly resolved spectrum is obtained (Figure 4b) consisting of two signals, one at 60 ppm with associated spinning sidebands and the other at 50 ppm. Their relative intensities are in the ratio of 4:1. No further changes are found at 250 °C, but after heating to 300 °C for 15 min and 370 °C for 10 min a multitude of narrow resonances are observed in the aliphatic region (−10 to +40 ppm) (Figure 4c,d). No other signals were found. Spectral deconvolution of these resonances is shown in Figure 5 while the molecular species assigned and their relative concentrations are listed in Table I. Deconvolution was performed by reference to literature values of $^{13}C$ NMR chemical shifts[25] taking into account the likelihood of a small susceptibility shift for aliphatic molecules in the adsorbed phase (which for saturated hydrocarbons in zeolites is never greater than 1.5 ppm).[15] Spectral assignments were greatly facilitated by the fact that most compounds give more than one NMR signal.

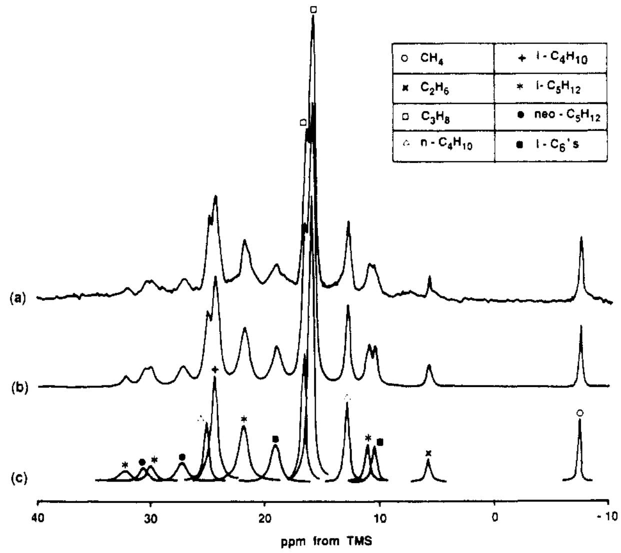

**Figure 5.** $^{13}C$ MAS NMR spectrum of the sample treated at 370 °C for 10 min (a) can be simulated (b) using $^{13}C$ signals corresponding to individual hydrocarbon species (c).

**TABLE I: Concentration of Aliphatic Species (in mol %) Detected in SAPO-34 by $^{13}C$ MAS NMR after Conversion of Methanol**

| | 300 °C | 370 °C |
|---|---|---|
| methane | 13.4 | 13.7 |
| ethane | 5.7 | 2.5 |
| propane | 18.7 | 35.9 |
| *n*-butane | 9.9 | 11.9 |
| isobutane | 14.8 | 11.7 |
| isopentane | 21.1 | 16.4 |
| neopentane | 3.1 | 2.5 |
| $C_6$ and higher | 13.2 | 5.3 |

After reaction at 300 °C, the most abundant species in the adsorbed phase are isopentane, propane, isobutane, methane, and *n*-butane with less ethane, neopentane, $C_6$, and $C_7$ species. After reaction at 370 °C, the composition of the adsorbed phase is similar except that propane is now more abundant than isopentane. The relative concentrations of adsorbed species were calculated from spectra acquired with high-power proton decoupling but without cross-polarization. We believe that spectral intensity problems associated with the nuclear Overhauser enhancement (NOE) are negligible as the decoupler was turned off during the recycle delay.[26] Unlike in the case of zeolite H-ZSM-5[12,13] no carbon monoxide intermediate and no aromatics are observed by NMR at any temperature.

The distributions of the gaseous products at various temperatures and space velocities (given as liquid hourly space velocity, LHSV, in liters of reactants per liter of catalyst per hour) are listed in Table II. At 128–168 °C MeOH is converted almost exclusively to dimethyl ether (DME). At 242 °C there is about 11% conversion to hydrocarbons, which at 300 °C and sufficiently low space velocities (below ca. 0.3 $h^{-1}$) increases to 100%. The major product is always ethane followed by ethylene, propylene, ethane, and propane. All $C_4$ and larger hydrocarbons are in very low abundance in the products. The concentration ratio of aliphatics to olefins increases greatly as the space velocity is lowered.

## Discussion

The framework structure of SAPO-34 consists of hexagonal prisms (D6R units) linked by four-membered rings in an ABC ABC packing sequence[27] (see Figure 1). This results in a

---

[24] Bennett, J. M.; Dytrych, W. J.; Pluth, J. J.; Richardson Jr., J. W.; Smith, J. V. *Zeolites* **1986**, *6*, 349.

[25] Kalinowski, H. O.; Berger, S.; Braun, S. *$^{13}C$-NMR-Spektroskopie*; Georg Thieme: Stuttgart, 1984.

[26] Harris, R. K. *Nuclear Magnetic Resonance Spectroscopy*; Longmans: New York, 1986.

[27] Meier, W. M.; Olson, D. H. *Atlas of Zeolite Structure Types*; Butterworths: Sevenoaks, Kent, 1988.

**TABLE II: Product Distributions for Conversion of Methanol over SAPO-34 for Different Values of LHSV and Temperature**[a]

| temp, °C | 128 | 140 | 168 | 242 | 300 | 300 | 300 | 363 | 358 |
|---|---|---|---|---|---|---|---|---|---|
| LHSV, $h^{-1}$ | 0.4 | 1.7 | 1.6 | 1.6 | 0.3 | 1.7 | 9.2 | 0.3 | 9.2 |
| methanol | 67.8 | 66.9 | 74.5 | 28.2 | traces | 53.4 | 41.2 |  | 57.1 |
| dimethyl ether | 32.2 | 33.1 | 25.3 | 71.8 | traces | 46.6 | 58.8 |  | 42.9 |
| total hydrocarbons, mol % | 0.1 | 0.1 | 0.3 | 11.0 | 98.6 | 67.7 | 13.8 | 100 | 49.1 |
| methane | traces |  | traces | 88.4 | 69.0 | 61.6 | 59.9 | 78.4 | 69.4 |
| ethylene | traces | traces | traces | 9.2 | 11.7 | 26.7 | 29.8 | 3.9 | 21.5 |
| ethane |  |  |  |  | 8.4 | 1.6 |  | 9.8 | 0.2 |
| propylene | traces | traces | traces | 2.2 | 3.2 | 7.1 | 9.1 | 1.8 | 7.4 |
| propane |  |  |  |  | 5.4 | 0.9 |  | 4.8 |  |
| isobutane |  |  |  |  |  |  |  | 0.04 |  |
| but-1-ene | traces | traces | traces | 0.1 | 0.2 | 0.3 | 0.2 | 0.2 | 0.2 |
| *n*-butane |  |  |  | traces | 0.8 | 0.2 | traces | 0.5 | 0.04 |
| *trans*-but-2-ene | traces | traces | traces | 0.1 | 0.6 | 0.8 | 0.8 | 0.3 | 0.7 |
| *cis*-but-2-ene | traces | traces | traces | 0.07 | 0.3 | 0.4 | 0.2 | 0.2 | 0.2 |
| $C_5$ | traces | traces |  | traces | 0.4 | 0.4 | 0.02 |  | 0.3 |
| $C_6$ |  |  |  | traces | traces | 0.04 |  | 0.1 | 0.1 |

[a] Both MeOH and DME distributions as well as hydrocarbon distributions are normalized to 100 mol %.

three-dimensional channel system and a structure containing large ellipsoidal cages 11 Å long and 6.5 Å wide. The cages are stacked in a hexagonal arrangement forming a three-dimensional network of cages linked by the narrower eight-membered windows. The cage and window dimensions for SAPO-34 are almost identical with those in chabazite, and therefore similar molecular sieving properties can be expected. Entrance to the chabazite cages may only be gained through the eight-membered ring windows which are nearly circular with a diameter of approximately 3.8 Å. At room temperature chabazite very rapidly sorbs $O_2$, $H_2$, $CH_4$, and $C_2H_6$, slowly sorbs *n*-alkanes, but completely excludes branched alkanes.[28-31]

The $^{13}C$ MAS NMR signals from the MeOH and DME adsorbed on SAPO-34 after thermal treatment at 150 °C are much broader (fwhm = 300 Hz) than in zeolite H-ZSM-5 (80 Hz)[12,13] (Figure 3a,b), suggesting either that MeOH and DME are more strongly bound or that strong residual dipole–quadrupole interactions between $^{13}C$ and $^{27}Al$ in the SAPO framework are present.[32,33] After conversion into hydrocarbons the aliphatic resonances are much narrower (ca. 40 Hz), which indicates that polar oxygenates are more strongly bound than nonpolar hydrocarbons.

The molar ratio of DME to MeOH in the adsorbed phase calculated from the intensities of the respective $^{13}C$ NMR signals at 150 °C is approximately 2:1. This is in good agreement with that found for products by gas chromatography at low space velocities and indicates that neither DME nor MeOH is preferentially adsorbed or prevented from leaving SAPO-34 by steric or diffusional restrictions.

$^{13}C$ MAS NMR indicates that after heating to 300 °C MeOH and DME are completely converted to aliphatic hydrocarbons; no olefins are found. This is easily understood by reference to Table II which shows that at lower space velocities the products contain a smaller amount of olefins. By extrapolating the data, we predict that under static reactor conditions little or no olefins will be formed. This is in agreement with earlier work on methanol conversion on H-ZSM-5[34] where the production of olefins is only favored at very high space velocities when there is insufficient time for hydrogenation to occur. However, this does not invalidate a direct comparison of the NMR and gas chromatography data. Careful inspection of Table II indicates that the relative amounts of $C_1$, $C_2$, $C_3$, $C_4$, etc., species (olefins + aliphatics) are roughly similar irrespective of space velocity. In other words, space velocity does not change oligomerization properties, but it does alter the extent of hydrogenation of products. Therefore, NMR results, which give a fair representation of the total concentration of species formed in the adsorbed phase, can be compared with the concentration in the gaseous products.

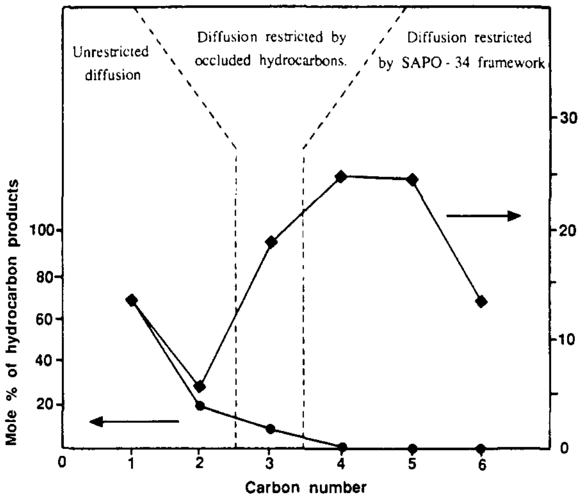

**Figure 6.** Plot of concentrations of $C_1$ to $C_6$ hydrocarbons at 300 °C in the gaseous products determined by gas chromatography (GC) and total hydrocarbons by NMR: ●, GC; ◆, NMR. GC data are for LHSV = 0.3 $h^{-1}$. NMR and GC data are adjusted so that the concentrations of methane coincide.

The most striking difference between the composition of the adsorbed phase and the products is the preponderance of branched aliphatics up to $C_6$ in the former. The effect is so clear as to amount to a textbook example of product shape selectivity. Early work in Barrer's laboratory has shown[28-31] that these branched aliphatics are not sorbed by the chabazite crystals from the gas phase at room temperature. Here we demonstrate the same effect in reverse: branched-chain hydrocarbons formed *inside* SAPO-34 are not capable of leaving the intracrystalline space even at temperatures as high as 370 °C.

Of the $C_1$, $C_2$, and $C_3$ species in the adsorbed phase the concentration of $C_3$ is always the highest. However, it is $C_1$ which is the most abundant in the gaseous products, followed by $C_2$ and $C_3$ species. The $C_1/C_2$ concentration ratio in the adsorbed phase is roughly equal to that in the gaseous products at 300 °C (compare Tables I and II). This suggests that $C_1$ and $C_2$ species have no difficulty in leaving the SAPO-34 crystallite. On the other hand, only 5–10% of the amount of $C_3$ found in the adsorbed phase is observed in the gas-phase products. Figure 6 illustrates the relative amounts of $C_1$–$C_6$ compounds in the products and in the adsorbed phase. The striking difference between the concentrations of $C_1$ and $C_2$ on the one hand and $C_3$ on the other is not easily explained on the basis of diffusion coefficients of aliphatic hydrocarbons in chabazite.[28-31] At room temperature the diffusion coefficient of propane is ca. 20 times smaller than for ethane and

---

(28) Barrer, R. M.; Ibbitson, D. A. *Trans. Faraday Soc.* **1944**, *40*, 195.
(29) Barrer, R. M.; Ibbitson, . A. *Trans. Faraday Soc.* **1944**, *40*, 206.
(30) Barrer, R. M.; Brook, D. W. *Trans. Faraday Soc.* **1953**, *49*, 1049.
(31) Barrer, R. M.; Davies, J. A. *Proc. R. Soc. London, A* **1971**, *322*, 1.
(32) Oppella, S. J.; Frey, M. H.; Cross, T. A. *J. Am. Chem. Soc.* **1979**, *101*, 5856.
(33) Anderson, M. W.; Klinowski, J. *J. Chem. Soc., Chem. Commun.*, submitted for publication.
(34) Chang, C. D.; Silvestri, A. J. *J. Catal.* **1977**, *47*, 249.
(35) Derouane, E. G.; Gabelica, Z. *J. Catal.* **1980**, *65*, 486.

methane. However, at elevated temperatures, such as 150 °C, the difference disappears almost completely. It follows that at 370 °C the expected diffusion coefficients for methane, ethane, and propane should be of the same order of magnitude with a negligible activation barrier. The exclusion of much of the $C_3$ fraction from the product must therefore be a result of the additional constraints imposed by the presence of branched hydrocarbons which partially block the pore system and significantly alter the diffusional behavior of other species. Such restrictions on reaction products are along the lines proposed by Derouane and Gabelica[35] for the counterdiffusion of reactants and products. The difference here is that in SAPO-34 the interfering species are trapped within the chabazite cages. This further illustrates the need for knowing the contents of the intracrystalline space of a shape-selective catalyst during the course of the reaction. Since the available free space is modified by the occlusion of product molecules, it is not sufficient to take into account the crystallographic pore dimensions in order to predict shape-selective action.

The discovery that, despite the composition of the gaseous products, SAPO-34 in fact converts methanol more selectively to $C_3$ than to $C_2$ hydrocarbons suggests ways to modify the catalyst so as to enable the $C_3$ species to escape, thus making it more selective for propylene than ethylene. This might be done by preparing the catalyst with occluded material or partial exchange with cations large enough to prevent the formation of branched hydrocarbons. This would in turn allow the $C_2$ and $C_3$ species to diffuse more readily through the channel system without obstruction from the higher hydrocarbons. The fact that such a prediction can be made on the strength of MAS NMR in tandem with gas chromatography ilustrates the remarkable potential of this two-pronged approach in the design of novel molecular sieve catalysts.

*Acknowledgment.* We are grateful to Shell Research, Amsterdam, for supporting the NMR measurements, to Unilever Research, Port Sunlight, for supporting the gas chromatography work, and to the SERC for a research studentship for P.J.B.

---

# Strong Circular Polarization in the Excimer Emission from a Pair of Pyrenyl Groups Linked to a Polypeptide Chain

**Yoshihito Inai,[†] Masahiko Sisido,* and Yukio Imanishi[†]**

*Department of Polymer Chemistry, Kyoto University, Sakyo-ku, Kyoto 606, Japan, and Research Laboratory of Resources Utilization, Tokyo Institute of Technology, 4259 Nagatsuta, Midori-ku, Yokohama 227, Japan*

*(Received: November 9, 1989)*

Very strong circular polarization was observed in the excimer emission from a pair of pyrenyl groups linked to an $\alpha$-helical polypeptide chain: H-Glu(OBzl)$_n$-pyrAla-Ala$_m$-pyrAla-Glu(OBzl)$_4$-OBzl. Strong right-circular polarization with $g_{em} = -0.016$ was detected for the polypeptide of $m = 0$, whereas strong left-circular polarization with $g_{em} = 0.016$ was detected for the polypeptide of $m = 2$. The relation between the screw sense of the excimer configuration and the sign of the circular polarization was discussed on the basis of the ground-state conformations of the pyrenyl groups. It was concluded that an excimer with a left-handed screw configuration emits left circularly polarized fluorescence.

## Introduction

Excimer formation has been used to probe the statics and the dynamics of the distribution of fluorescent-labeled molecules in biological systems,[1] polymer systems,[2] liquid crystals,[3] and other molecular organizates. However, the geometry of the excimer configuration has not been discussed in detail in the past. This may be due to the lack of an appropriate spectroscopic technique and appropriate model compounds that have definite excimer configurations. For chiral systems, circularly polarized fluorescence (CPF) spectroscopy[4] provides information on the structure of excited-state species. CPF spectra have been reported for the excimers in polypeptides carrying 2-naphthyl, 9-anthryl,[5] and 1-pyrenyl[6] chromophores and in pyrene–$\gamma$-cyclodextrin inclusion complexes.[7] Although positive or negative CPF signals have been detected for those excimer emissions, no relation between the sign of the CPF signal and the screw sense of the excimer configuration has been established yet. In this study, an attempt was made to correlate the screw sense with the sign of CPF signal using the polypeptides I ($m$ = 0, 2).

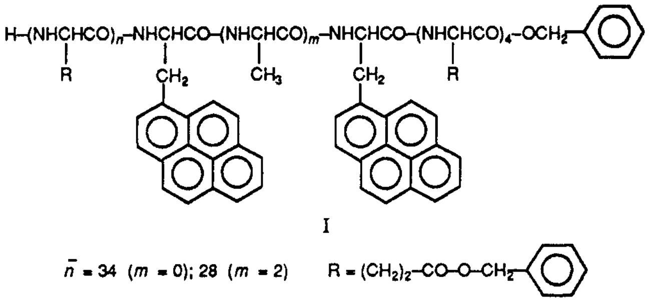

I

[Glu(OBzl)$_n$–pyrAla–Ala$_m$–pyrAla–Glu(OBzl)$_4$–OBzl]

## Experimental Section

The polypeptide was synthesized by a polymerization of $\gamma$-benzyl L-glutamate $N$-carboxyanhydride using a hexapeptide, H-pyrAla$_2$-Glu(OBzl)$_4$-OBzl, or an octapeptide, H-pyrAla-Ala$_2$-pyrAla-Glu(OBzl)$_4$-OBzl, as the initiator [pyrAla = L-1-pyrenylalanine, Glu(OBzl) = $\gamma$-benzyl L-glutamate, Ala = L-alanine, OBzl = $O$-benzyl ester]. The initiators were synthesized by the stepwise liquid-phase method. The oligopeptides were

---

* Correspondence should be addressed to this author at Tokyo Institute of Technology.

[†] Kyoto University.

(1) (a) Galla, H.-J.; Sachman, E. *Biochim. Biophys. Acta* **1973**, *339*, 103. (b) Dembo, M.; Glushko, V.; Aberlin, M. E.; Sonenberg, M. *Biochim. Biophys. Acta* **1979**, *522*, 201. (c) Soutar, A. K.; Pownall, H. J.; Hu, A. S.; Smith, L. C. *Biochemistry* **1974**, *13*, 2828. (d) Otoyo, T.; Shimagaki, M.; Otoda, K.; Kimura, S.; Imanishi, Y. *Biochemistry* **1988**, *27*, 6458. (e) Mihara, H.; Lee, S.; Shimohigashi, Y.; Aoyagi, H.; Kato, T.; Izumiya, N.; Costa, T. *Int. J. Peptide Protein Res.* **1987**, *30*, 605.

(2) (a) Winnik, M. A. *Acc. Chem. Res.* **1985**, *18*, 73. (b) Hoyle, C. E.; Torkelson, J. M., Eds. *Photophysics of Polymers*; ACS Symposium Series 358; American Chemical Society: Washington, DC, 1987.

(3) (a) Sisido, M.; Wang, X.-F.; Kawaguchi, K.; Imanishi, Y. *J. Phys. Chem.* **1988**, *92*, 4797. (b) Anderson, V. C.; Craig, B. B.; Weiss, R. G. *J. Am. Chem. Soc.* **1981**, *103*, 7169; *J. Phys. Chem.* **1982**, *86*, 4642.

(4) Riehl, J. P.; Richardson, F. S. *Chem. Rev.* **1986**, *86*, 1.

(5) Sisido, M.; Egusa, S.; Okamoto, A.; Imanishi, Y. *J. Am. Chem. Soc.* **1983**, *105*, 3351.

0022-3654/90/2094-2734$02.50/0